



Substituent dependent dimensionalities in cobalt isophthalate supramolecular complexes and coordination polymers containing dipyridylamine ligands

Jacqueline S. Lucas, Lestella D. Bell, Chaun M. Gandolfo, Robert L. LaDuca *

Lyman Briggs College and Department of Chemistry, Michigan State University, East Lansing, MI 48825, USA

ARTICLE INFO

Article history:

Received 18 March 2011
Received in revised form 25 August 2011
Accepted 2 September 2011
Available online 21 September 2011

Keywords:

Hydrothermal synthesis
Cobalt
Isophthalate
Coordination polymer
Dipyridylamine
Thermogravimetric analysis

ABSTRACT

Hydrothermal synthesis has afforded cobalt 5-substituted isophthalate complexes with 4,4'-dipyridylamine (dpa) ligands, showing different dimensionalities depending on the steric bulk and hydrogen-bonding ability of the substituent. $[\text{Co}(t\text{Buip})(\text{dpa})(\text{H}_2\text{O})]_n$ (**1**, *t*Buip = 5-*tert*-butylisophthalate) is a (4,4) grid two-dimensional coordination polymer featuring 2-fold parallel interpenetration. $[\text{Co}(\text{MeOip})_2(\text{Hdpa})_2]_n$ (**2**, MeOip = 5-methoxyisophthalate) is organized into 3-fold parallel interpenetrated (4,4) grids through strong $\text{N}-\text{H}^+\cdots\text{O}^-$ hydrogen bonding. $\{[\text{Co}(\text{OHip})(\text{dpa})(\text{H}_2\text{O})_3]_3\cdot 2\text{H}_2\text{O}\}_n$ (**3**, OHip = 5-hydroxyisophthalate) possesses 1-D chain motifs. The 5-methyl derivative $\{[\text{Co}(\text{mip})(\text{dpa})]_3\cdot 3\text{H}_2\text{O}\}_n$ (**4**, mip = 5-methylisophthalate) has a 3-D 6^38 cds topology. $\{[\text{Co}(\text{H}_2\text{O})_4(\text{Hdpa})_2](\text{nip})_2\cdot 2\text{H}_2\text{O}\}_n$ (**5**, nip = 5-nitroisophthalate) and $\{[\text{Co}(\text{sip})(\text{Hdpa})(\text{H}_2\text{O})_4]\cdot 2\text{H}_2\text{O}\}_n$ (**6**, sip = 5-sulfoisophthalate) are coordination complexes. Antiferromagnetic superexchange is observed in **1** and **4**, with concomitant zero-field splitting. Thermal decomposition behavior of the higher dimensionality complexes is also discussed.

© 2011 Elsevier B.V. All rights reserved.

1. Introduction

Coordination polymer crystalline solids, constructed from the linkage of metal ions through anionic and neutral organic ligands, may have important industrial applications [1] including gas storage [2], absorption and separation [3], cation or anion exchange [4], catalysis [5], guest-dependent luminescence [6], and in non-linear optical devices [7]. Anionic aromatic dicarboxylates such as terephthalate [8] or isophthalate (ip) [9] have been frequently used as linking ligands towards the construction of divalent metal coordination polymers, through their ability to stabilize a neutral crystalline framework. A synergism between divalent metal ion coordination environment, carboxylate group position, carboxylate binding or bridging modes and the presence of any dipyridyl coligands [10] is responsible for the supramolecular arrangement during self-assembly. Therefore any *a priori* prediction of coordination polymer structure can remain elusive. In coordination polymer solids containing divalent cobalt ions, the presence of multinuclear clusters can cause temperature-dependent or field-dependent magnetic behavior such as spin-canting and single-chain magnetism [11].

Substituted isophthalate ligands such as 5-hydroxyisophthalate (OHip) [12–15], 5-methoxyisophthalate (OMeip) [16,17], 5-nitroisophthalate (nip) [18–22], 5-*tert*-butylisophthalate (*t*Buip) [23], 5-methylisophthalate (mip) [24,25], or 5-sulfoisophthalate (sip)

[26] have been seeing more recent use in coordination polymer chemistry, in order to evaluate the effect of the substituent on structural topology and the resulting influence on physical properties. For instance, $\{[\text{Co}(\text{OHip})(\text{dpp})]_3\cdot \text{H}_2\text{O}\}_n$ (dpp = 1,3-di(4-pyridyl)propane) shows a 4-fold interpenetrated diamondoid topology, while its nickel derivative $[\text{Ni}(\text{OHip})(\text{dpp})_{1.5}(\text{H}_2\text{O})]_n$ displays interdigitated sets of 1-D ribbon motifs [12]. The 3-D network material $[\text{Zn}(t\text{Buip})]_n$ (*t*Buip = 5-*tert*-butylisophthalate) synthesized by Li et al. contains 1-D solvent-free channels that permit the separation of methanol from water [23]. A recent unique example of 2-fold interpenetration of self-penetrated **mab** 4^46^{108} topology networks was seen in a zinc mip coordination polymer with a very long dipyridylbenzamide ligand [24]. $[\text{Cu}_4(\text{OH})_2(\text{sip})_2(2,2'\text{-bipyridine})_2(\text{H}_2\text{O})_2]_n$ and $\{[\text{Cu}_4(\text{OH})_2(\text{sip})_2(\text{H}_2\text{O})_2]\cdot 4\text{H}_2\text{O}\}_n$ adopt uncommon 3-D $(4.6^2)_2(4^26^{108^3})$ rutile and $(4^56)_2(4^{116^{148^3}})$ fluorite variant networks, respectively [26a].

Solid solutions of substituted isophthalate coordination polymers can also perform useful separations, as discovered Kitagawa et al. in a recent study [27]. Crystalline solid solutions of the layered phase $\{[\text{Zn}(\text{nip})(4,4'\text{-bpy})](0.5\text{DMF}\cdot 0.5\text{MeOH})\}_n$ with its isostructural MeOip analog can be tailored in order to change the gate-opening pressure for water adsorption. Additionally, CO_2 absorption selectivity can be increased by adjusting the number of MeOip ligands in the solid solution.

Although there has been some recent exploratory synthesis of substituted isophthalate coordination polymer phases, studies that systematically investigate size-dependent steric effects imposed by these substituents have been less common. Yang et al. showed

* Corresponding author.

E-mail address: laduca@msu.edu (R.L. LaDuca).

that increasing steric hindrance caused a decrease in coordination polymer dimensionality in a system with monodentate pyridine coligands [28]. $[\text{Zn}_4(\text{H}_2\text{O})(\text{ip})_4(\text{py})_6]_n$ (py = pyridine), $\{[\text{Zn}_2(\text{OHip})_2(\text{py})_4]_2(\text{py})_n\}$, and $[\text{Zn}(\text{tBuip})(\text{py})_2]_n$ show 2-D grid-like layers, 1-D single-stranded chains, and 1-D double-stranded ribbons, respectively. We were recently able to corroborate this apparent trend in a system with the long-spanning tethering ligand bis(4-pyridylformyl)piperazine (bfpf) [29]. $\{[\text{Cu}(\text{ip})(4\text{-bfpf})\cdot 2\text{H}_2\text{O}]_n\}$ has a (4,4) rectangular grid structure, while $[\text{Cu}_2(\text{tBu ip})_2(4\text{-bfpf})(\text{H}_2\text{O})_2]_n$ and $\{[\text{Cu}(\text{MeOip})(\text{HMeOip})_2(4\text{-bfpf})\cdot 3\text{H}_2\text{O}]_n\}$ display 1-D ladder and chain motifs, respectively.

The angular disposition of the pyridyl nitrogen donor atoms and central hydrogen bonding point of contact within 4,4'-dipyridylamine (dpa) has provided access to many new coordination polymer topologies in aliphatic or aromatic dicarboxylate systems [30–32]. For example, $\{[\text{Ni}(\text{dpa})_2(\text{succinate})_{0.5}\text{Cl}]_n\}$ possesses a unique self-penetrated regular (6,5) 3-D network with 6¹⁰ **rdl-z** topology [30]. $\{[\text{Cd}(\text{phthalate})(\text{dpa})(\text{H}_2\text{O})\cdot 4\text{H}_2\text{O}]_n\}$ has an unprecedented 4-connected uninodal self-penetrated three-dimensional 7⁴8² topology (**yyz** net), constructed from the interlocking of $[\text{Cd}(\text{dpa})]_n$ double helices with $[\text{Cd}(\text{pht})]_n$ single helices [31]. To date, however, there have been no reports of coordination polymers containing both dpa and substituted isophthalate ligands. In this study we report the preparation and structural characterization of $[\text{Co}(\text{tBuip})(\text{dpa})(\text{H}_2\text{O})]_n$ (**1**), $[\text{Co}(\text{MeOip})_2(\text{Hdpa})_2]_n$ (**2**), $\{[\text{Co}(\text{OHip})(\text{dpa})(\text{H}_2\text{O})_3]_3\cdot 2\text{H}_2\text{O}\}_n$ (**3**), $\{[\text{Co}(\text{mip})(\text{dpa})\cdot 2\text{H}_2\text{O}]_n\}$ (**4**), $\{[\text{Co}(\text{H}_2\text{O})_4(\text{Hdpa})_2(\text{nip})_2\cdot 2\text{H}_2\text{O}\}_n$ (**5**, nip = 5-nitroisophthalate) and $\{[\text{Co}(\text{sip})(\text{Hdpa})(\text{H}_2\text{O})_4]_2\cdot 2\text{H}_2\text{O}\}_n$ (**6**, sip = 5-sulfoisophthalate) whose dimensionalities and topologies differ greatly from each other, depending on the nature of the 5-position substituent. Thermal decomposition behavior of the higher dimensionality complexes is also presented, along with the variable temperature magnetic susceptibility of **1** and **4** because of their closely spaced cobalt ions.

2. Experimental

2.1. General considerations

Cobalt salts and substituted isophthalic acids were commercially obtained. 4,4'-Dipyridylamine was synthesized using a published procedure [33]. Water was deionized above 3 MΩ-cm in-house. Elemental analysis was carried out using a Perkin–Elmer 2400 Series II CHNS/O Analyzer. IR spectra were recorded on powdered samples using a Perkin–Elmer Spectrum One instrument. Thermogravimetric analysis was performed on a TA Instruments high-resolution Q500 thermal analyzer under flowing N₂. Variable temperature magnetic susceptibility data (2–300 K) for **1** was collected on a Quantum Design MPMS SQUID magnetometer at an applied field of 0.1 T. After each temperature change the sample was kept at the new temperature for 5 min before magnetization measurement to ensure thermal equilibrium. The susceptibility data was corrected for diamagnetism using Pascal's constants [34] and for the diamagnetism of the sample holder.

2.2. Preparation of $[\text{Co}(\text{tBuip})(\text{dpa})(\text{H}_2\text{O})]_n$ (**1**)

Cobalt nitrate hexahydrate (108 mg, 0.37 mmol), dpa (63 mg, 0.37 mmol), 5-*tert*-butylisophthalic acid (72 mg, 0.37 mmol) and 10 mL deionized water were placed into a 23 mL Teflon-lined acid digestion bomb. The bomb was sealed and heated in an oven at 120 °C for 48 h, and then cooled slowly to 25 °C. Pink blocks of **1** (66 mg, 38% yield based on Co) were isolated after washing with distilled water, ethanol, and acetone and drying in air. *Anal. Calc.* for C₄₄H₄₆Co₂N₆O₁₀ (**1**): C, 56.42; H, 4.95; N, 8.97. Found: C,

56.01; H, 4.72; N, 8.86%. IR (cm⁻¹): 3400 (w, br), 2949 (w), 1598 (s), 1562 (w), 1523 (s), 1438 (m), 1355 (s), 1214 (s), 1016 (s), 910 (m), 847 (w), 806 (s), 777 (m), 726 (s), 692 (w).

2.3. Preparation of $[\text{Co}(\text{MeOip})_2(\text{Hdpa})_2]_n$ (**2**)

Cobalt nitrate hexahydrate (108 mg, 0.37 mmol), dpa (63 mg, 0.37 mmol), 5-methoxyisophthalic acid (72 mg, 0.37 mmol) and 10 mL deionized water were placed into a 23 mL Teflon-lined acid digestion bomb. The bomb was sealed and heated in an oven at 120 °C for 48 h, and then cooled slowly to 25 °C. Purple needles of **2** (16 mg, 5% yield based on Co) were isolated after manual separation from unreacted organics, washing with distilled water, hot ethanol, and acetone and drying in air. *Anal. Calc.* for C₃₈H₃₂CoN₆O₁₀ (**2**): C, 57.65; H, 4.07; N, 10.62. Found: C, 57.28; H, 3.83; N, 10.40%. IR (cm⁻¹): 3380 (w), 3108 (w), 1692 (w), 1643 (w), 1595 (w), 1568 (m), 1525 (s), 1445 (m), 1363 (s), 1288 (w), 1247 (w), 1208 (m), 1122 (w), 1056 (s), 1013 (s), 910 (w), 972 (w), 835 (w), 814 (m), 763 (s), 703 (s), 680 (w).

2.4. Preparation of $\{[\text{Co}(\text{OHip})(\text{dpa})(\text{H}_2\text{O})_3]_3\cdot 2\text{H}_2\text{O}\}_n$ (**3**)

Cobalt nitrate hexahydrate (110 mg, 0.377 mmol), dpa (62 mg, 0.37 mmol), 5-hydroxyisophthalic acid (62 mg, 0.34 mmol), 2 mL of 1.0 M NaOH solution, and 10 mL deionized water were placed into a 23 mL Teflon-lined acid digestion bomb. The bomb was sealed and heated in an oven at 120 °C for 48 h, and then cooled slowly to 25 °C. Pink blocks of **3** (33 mg, 20% yield based on 5-hydroxyisophthalic acid) were isolated after manual separation from unreacted organics, washing with distilled water, hot ethanol, and acetone and drying in air. *Anal. Calc.* for C₅₄H₆₁Co₃N₉O₂₆ (**3**): C, 45.39; H, 4.30; N, 8.82. Found: C, 46.10; H, 3.91; N, 9.10%. IR (cm⁻¹): 2961 (w), 1595 (vs), 1556 (vs), 1514 (vs), 1400 (vs), 1367 (vs), 1351 (vs), 1299 (m), 1269 (m), 1213 (m), 1132 (w), 1094 (w), 1064 (w), 1017 (m), 973 (w), 844 (m), 818 (vs), 784 (vs), 718 (s).

2.5. Preparation of $\{[\text{Co}(\text{mip})(\text{dpa})\cdot 3\text{H}_2\text{O}]_n\}$ (**4**)

Cobalt nitrate hexahydrate (103 mg, 0.35 mmol), dpa (59 mg, 0.35 mmol), 5-methylisophthalic acid (62 mg, 0.34 mmol), 2 mL of 1.0 M NaOH solution, and 10 mL deionized water were placed into a 23 mL Teflon-lined acid digestion bomb. The bomb was sealed and heated in an oven at 150 °C for 48 h, and then cooled slowly to 25 °C. Magenta blocks of **4** (69 mg, 44% yield based on 5-methylisophthalic acid) were isolated after manual separation from unreacted organics, washing with distilled water, hot ethanol, and acetone and drying in air. *Anal. Calc.* for C₁₉H₂₁CoN₃O₇ (**4**): C, 49.36; H, 4.58; N, 9.09. Found: C, 49.90; H, 3.73; N, 9.12%. IR (cm⁻¹): 3651 (w), 3281 (w), 3175 (w), 3067 (w), 1615 (w), 1580 (m), 1547 (w), 1523 (s), 1442 (w), 1424 (m), 1383 (s), 1349 (m), 1252 (w), 1214 (m), 1115 (w), 1060 (w), 1017 (s), 951 (w), 926 (w), 905 (w), 838 (w), 811 (m), 797 (m), 774 (s), 723 (s), 665 (w).

2.6. Preparation of $\{[\text{Co}(\text{H}_2\text{O})_4(\text{Hdpa})_2(\text{nip})_2\cdot 2\text{H}_2\text{O}]_n\}$ (**5**)

Cobalt nitrate hexahydrate (102 mg, 0.35 mmol), dpa (61 mg, 0.35 mmol), 5-nitroisophthalic acid (77 mg, 0.36 mmol), 2 mL of 1.0 M NaOH solution, and 10 mL deionized water were placed into a 23 mL Teflon-lined acid digestion bomb. The bomb was sealed and heated in an oven at 120 °C for 48 h, and then cooled slowly to 25 °C. Pink needles of **5** (63 mg, 39% yield based on dpa) were isolated after manual separation from unreacted organics, washing with distilled water, hot ethanol, and acetone and drying in air. *Anal. Calc.* for C₃₆H₃₈CoN₈O₁₈ (**5**): C, 46.51; H, 4.12; N, 12.05. Found: C, 46.58; H, 3.86; N, 11.80%. IR (cm⁻¹): 3098 (w), 1646

(w), 1599 (m), 1560 (m), 1532 (m), 1518 (m), 1426 (w), 1337 (vs), 1204 (m), 1094 (w), 1079 (w), 1062 (w), 1014 (w), 973 (w), 921 (w), 847 (w), 825 (m), 788 (m), 723 (s).

2.7. Preparation of $\{[Co(sip)(Hdpa)(H_2O)_4] \cdot 2H_2O\}_n$ (**6**)

Cobalt sulfate hexahydrate (83 mg, 0.32 mmol), dpa (34 mg, 0.20 mmol), sodium 5-sulfoisophthalate (53 mg, 0.20 mmol), 1.0 mL of 1.0 M NaOH, and 10 mL deionized water were placed into a 23 mL Teflon-lined acid digestion bomb. The bomb was sealed and heated in an oven at 120 °C for 48 h, and then cooled slowly to 25 °C. Magenta blocks of **6** (74 mg, 64% yield based on Co) were isolated after manual separation from unreacted organics, washing with distilled water, hot ethanol, and acetone and drying in air. Anal. Calc. for $C_{18}H_{25}CoN_3O_{13}S$ (**6**): C, 37.12; H, 4.33; N, 7.21. Found: C, 36.91; H, 4.12; N, 7.19%. IR (cm^{-1}): 3302 (w, br), 2516 (w, br), 2091 (w), 1643 (w), 1601 (s), 1545 (m), 1505 (s), 1474 (w), 1428 (s), 1361 (s), 1338 (s), 1199 (s), 1105 (s), 1043 (s), 1019 (m), 991 (w), 953 (w), 903 (w), 842 (w), 822 (s), 777 (s), 713 (s), 670 (w).

3. X-ray crystallography

Reflection data for **1–6** were collected on a Bruker-AXS SMART-CCD X-ray diffractometer using graphite-monochromated MoK α radiation ($\lambda = 0.71073 \text{ \AA}$). The data were processed via SAINT [35], and subjected to Lorentz and polarization effect and absorption corrections using SADABS [36]. The structures were solved using direct methods with SHELXTL [37]. The crystal of **5** was non-merohedrally twinned. Its twin law was found using CELLNOW [38], and only reflections from the major twin component was used. All non-hydrogen atoms were refined anisotropically. Hydrogen atoms bound to carbon were placed in calculated positions and refined isotropically with a riding model. Hydrogen atoms bound to the dpa central amine and protonated pyridyl groups and ligated water molecules were found by Fourier difference map where possible. Water molecule disorder in **3**, **5**, and **6** was modeled using partial occupancies. Crystallographic details for **1–6** are given in Table 1.

4. Results and discussion

4.1. Synthesis and Infrared Spectroscopy

Compounds **1–6** were prepared as crystalline solids by hydrothermal reaction of a cobalt salt with dpa and the appropriate 5-substituted isophthalic acid. An examination of each sample under a microscope showed only pink blocks for **1**, magenta rhombs for **2**, pink blocks for **3**, magenta blocks for **4**, pink needles for **5**, and magenta blocks for **6**. The infrared spectra of **1–6** were consistent with the components seen in their crystal structures. Features corresponding to pyridyl or phenyl ring flexing and puckering modes were observed in the region between 600 and 820 cm^{-1} . Medium intensity bands in the range of ~ 1600 to ~ 1200 cm^{-1} arise from stretching modes of the aromatic rings of the dicarboxylate ligands and pyridyl rings within the dpa ligands [39]. Asymmetric and symmetric C–O stretching modes of the benzenedicarboxylate moieties were evidenced by very strong, slightly broadened bands at 1523 and 1355 cm^{-1} for **1**, 1525 and 1363 cm^{-1} for **2**, 1514 and 1351 cm^{-1} for **3**, 1523 and 1383 cm^{-1} for **4**, 1518 and 1337 cm^{-1} for **5**, and 1505 and 1361 cm^{-1} for **6**. Weak, broad spectral features in the region of ~ 3400 cm^{-1} represent O–H stretching modes within the aqua ligands in **1** and **3–6**, and the N–H stretching mode for dpa central amine in **1–6**. An intense band at 1204 cm^{-1} in the spectrum of **5** is attributed to the N–O stretching modes of the nitro substituents in the nip ligands. The sulfonate substituents

within the sip ligands give rise to an intense feature at 1199 cm^{-1} in the spectrum of **6**.

4.2. Structural description of $[Co(tBuip)(dpa)(H_2O)]_n$ (**1**)

The asymmetric unit of compound **1** contains two crystallographically distinct cobalt atoms, two *t*Buip ligands, two dpa ligands, and two aqua ligands. The coordination environment at each cobalt atom is a distorted $\{CoO_4N_2\}$ octahedron, with a chelating *t*Buip carboxylate group, a monodentate *t*Buip carboxylate group (Fig. 1), and a dpa pyridyl nitrogen donor occupying equatorial sites. A dpa pyridyl nitrogen donor atom and an aqua ligand take up the axial positions. Thus at each cobalt atom, dpa pyridyl donors are oriented in a *cis* disposition. Bond lengths and angles within the coordination sphere are given in Table S2.

Cobalt atoms in **1** are connected into $[Co(tBuip)(H_2O)]_n$ chains that are oriented parallel to the *b* crystal direction. Crystallographically distinction between the chains is enforced by differences in the torsion of the carboxylate groups relative to the *t*Buip aromatic ring planes. In one type of *t*Buip ligand, these torsion angles are 5.4° and 19.2°, while in the other they are less twisted, measuring 3.2° and 17.1°. Adjacent $[Co(tBuip)(H_2O)]_n$ chains are connected by dpa ligands into (4,4) grid $[Co(tBuip)(dpa)(H_2O)]_n$ coordination polymer layers (Fig. 2). The dpa ligands bridge Co··Co distances of 11.833 or 11.868 Å, with slightly difference inter-ring torsions (13.2° or 12.1°, respectively).

Large windows within an undulating (4,4) $[Co(tBuip)(dpa)(H_2O)]_n$ layer, as defined by through-space Co··Co contact distances of ~ 14.8 and 16.2 Å, permit parallel $2d + 2d \rightarrow 2D$ interpenetration of an identical layer. Hydrogen bonding donation (Table S2) from the dpa amine functional groups in one layer to unligated carboxylate oxygen atoms in the other serves to stabilize the interpenetrated structure. The sterically bulky *tert*-butyl substituents project above and below each individual layer, fitting into pockets bracketed by *tert*-butyl groups belonging to the other layer.

Interpenetrated layer pairs stack along the *a* direction (Fig. 3), anchored by hydrogen bonding donation (Table S1) from the aqua ligands in one layer to ligated oxygen atoms within monodentate *t*Buip carboxylate groups and also oxygen atoms within chelating *t*Buip carboxylate groups in the other layer. The Co··Co distances across the pairwise Co–O–H··O–Co supramolecular contacts measure 4.936 Å (Fig. 4). Aromatic rings of the *t*Buip ligands in adjacent layer pairs engage in π – π stacking interactions (3.67 Å centroid-to-centroid distance), serving a supporting structure stabilizing role.

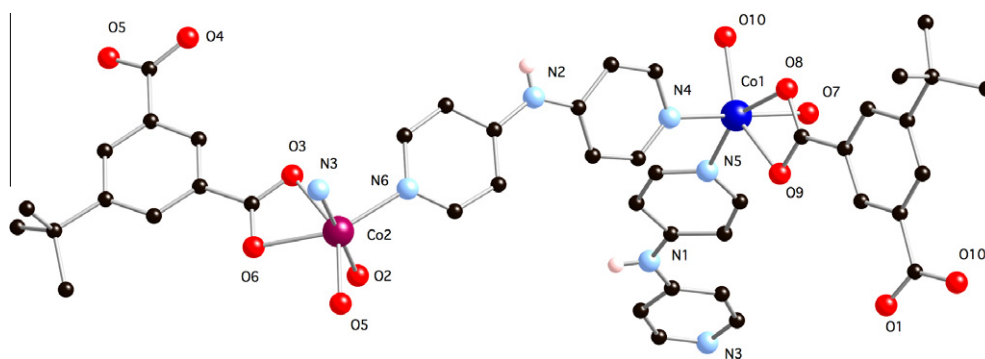
The interpenetrated layer structure of **1** contrasts greatly with its 3-D unsubstituted isophthalate (ip) analog $\{[Co(ip)(dpa)] \cdot 3H_2O\}_n$ [40]. This material possesses orthogonally arranged sets of parallel 1-D $[Co(ip)]_n$ chains bearing *anti-syn* bridged $\{Co(OCO)_2\}$ dinuclear units, pillared by dpa ligands into a 3-D 4-connected 6^58 cds topology network (Fig. 5). It is likely that the steric hindrance imparted by the 5-position *tert*-butyl groups in the *t*Buip ligands of **1** prevents aggregation into a 3-D coordination polymer lattice. This result corroborates the dimensionality-reducing trend caused by bulkier 5-position substituents seen previously by Wang and co-workers [28] and our group [29].

4.3. Structural description of $[Co(MeOip)_2(Hdpa)]_n$ (**2**)

The asymmetric unit of compound **2** contains a cobalt atom on a crystallographic 2-fold axis, one MeOip ligand, and a dpa molecule protonated at one of its pyridyl rings. Operation of the crystallographic 2-fold axis results in a complete neutral $[Co(MeOip)_2(Hdpa)_2]$ coordination complex, in which a distorted $\{CoO_2N_2\}$ tetrahedral geometry is present (Fig. 6). Bond lengths and angles within the coordination sphere are listed in Table S3.

Table 1
Crystal and Structure refinement data for 1–6.

Data	1	2	3	4	5	6
Formula	C ₄₄ H ₄₆ Co ₂ N ₆ O ₁₀	C ₃₈ H ₃₂ CoN ₆ O ₁₀	C ₅₄ H ₆₁ Co ₃ N ₉ O ₂₆	C ₁₉ H ₂₁ CoN ₃ O ₇	C ₃₆ H ₃₈ CoN ₆ O ₁₈	C ₁₈ H ₂₅ CoN ₃ O ₁₃ S
Formula weight	936.73	791.63	1428.91	462.32	929.67	582.40
Crystal system	monoclinic	monoclinic	monoclinic	monoclinic	triclinic	monoclinic
Space group	<i>P</i> 2 ₁ / <i>c</i>	<i>C</i> 2/ <i>c</i>	<i>P</i> 2 ₁ / <i>c</i>	<i>C</i> 2/ <i>c</i>	<i>P</i> $\bar{1}$	<i>P</i> 2 ₁
<i>a</i> (Å)	23.7681(15)	25.790(9)	18.176(2)	15.7443(9)	7.9028(11)	8.2251(17)
<i>b</i> (Å)	18.6018(12)	9.139(3)	14.0057(18)	12.7077(7)	13.8666(19)	17.033(4)
<i>c</i> (Å)	9.9930(6)	17.161(5)	24.547(3)	21.1794(12)	18.278(3)	8.4919(18)
α (°)	90	90	90	90	90.689(2)	90
β (°)	93.781(1)	122.83(2)	111.181(1)	103.919(1)	91.289(2)	91.731(2)
γ (°)	90	90	90	90	97.937(2)	90
<i>V</i> (Å ³)	4408.6(5)	3399(2)	5826.8(13)	4113.0(4)	1983.1(5)	1189.1(4)
<i>Z</i>	4	4	4	8	2	2
<i>D</i> (g cm ⁻³)	1.411	1.547	1.629	1.493	1.557	1.627
μ (mm ⁻¹)	0.816	0.578	0.941	0.881	0.523	0.882
Crystal size (mm)	0.28 × 0.20 × 0.18	0.40 × 0.10 × 0.10	0.41 × 0.18 × 0.16	0.45 × 0.22 × 0.20	0.58 × 0.10 × 0.04	0.36 × 0.19 × 0.16
Minimum/ maximum transmission	0.8061/0.8697	0.8014/0.9466	0.6995/0.8671	0.6921/0.8456	0.7525/0.9773	0.7407/0.8688
<i>hkl</i> Ranges	−28 ≤ <i>h</i> ≤ 28, −22 ≤ <i>k</i> ≤ 22, −12 ≤ <i>l</i> ≤ 12	−30 ≤ <i>h</i> ≤ 30, −10 ≤ <i>k</i> ≤ 10, −20 ≤ <i>l</i> ≤ 20	−21 ≤ <i>h</i> ≤ 21, −16 ≤ <i>k</i> ≤ 16, −29 ≤ <i>l</i> ≤ 29	−18 ≤ <i>h</i> ≤ 19, −15 ≤ <i>k</i> ≤ 15, −25 ≤ <i>l</i> ≤ 25	−9 ≤ <i>h</i> ≤ 9, −16 ≤ <i>k</i> ≤ 16, 0 ≤ <i>l</i> ≤ 21	−9 ≤ <i>h</i> ≤ 9, −20 ≤ <i>k</i> ≤ 20, −9 ≤ <i>l</i> ≤ 10
Total reflections	32022	13588	42146	14864	30694	7063
Unique reflections	8057	3088	10674	3812	7175	3886
<i>R</i> _{int}	0.0680	0.0797	0.0462	0.0277	0.0871	0.0209
Parameters/ restraints	583/6	257/1	911/39	285/3	619/22	370/18
<i>R</i> ₁ ^a (all data)	0.0854	0.1104	0.0675	0.0490	0.1354	0.0308
<i>R</i> ₁ ^a [<i>I</i> > 2σ(<i>I</i>)]	0.0610	0.0828	0.0430	0.0419	0.0607	0.0299
<i>wR</i> ₂ ^b (all data)	0.1739	0.2279	0.1197	0.1223	0.1314	0.0812
<i>wR</i> ₂ ^b [<i>I</i> > 2σ(<i>I</i>)]	0.1534	0.2090	0.1052	0.1169	0.1120	0.0802
Maximum/ minimum residual (e Å ⁻³)	0.905/−0.952	0.877/−0.612	0.875/−0.743	0.852/−0.579	0.361/−0.638	0.755/−0.253
Goodness-of-fit (GOF) on <i>F</i> ²	1.071	1.058	1.038	1.061	0.981	1.046

^a $R_1 = \sum ||F_o| - |F_c|| / \sum |F_o|$.^b $wR_2 = \{ \sum [w(F_o^2 - F_c^2)^2] / \sum [wF_o^2]^2 \}^{1/2}$.**Fig. 1.** Coordination environment of 1, shown with 50% thermal ellipsoids and atom numbering scheme. Hydrogen atoms have been omitted.

Individual [Co(MeOip)₂(Hdpa)₂] coordination complexes are linked into a supramolecular (4,4) grid structure by charge-separated ionic-character N⁺–H···O[−] hydrogen bonding (N···O3 distance = 2.609(6) Å) distance between the protonated pendant pyridyl groups of the dpa ligands and unligated MeOip carboxylate termini (Table S2). The long N–H bond distance (1.32(6) Å) is ascribed to the electrostatic attraction on the part of the negatively charged MeOip carboxylate oxygen. While this strong intermolecular interaction in **2** is best considered to be a N⁺–H···O[−] electrostatic-type attraction, some quasi-covalent N–H···O character can be invoked [41]. Hydrogen bonding has been referred to as “incipient proton transfer” [42], with these interactions in **2** being an example.

The very large 27.4 × 29.1 Å apertures in a single supramolecular layer, as measured by Co···Co through-space distances, allow interpenetration of two other identical [Co(MeOip)₂(Hdpa)₂]_n supramolecular nets (Fig. 7). The interpenetration of the individual rhomboid grid layers is fostered by C–H···O non-classical hydrogen bonding (C···O distance = 3.338(4) Å) between Hdpa pyridyl rings and the unligated oxygen atoms of the MeOip monodentate carboxylate groups. The pyridyl rings of the Hdpa ligands undergo a slight twist in order to optimize these interactions, with a dihedral angle of 11.9° between the ring planes.

The resulting 3-fold parallel interpenetrated network in **2** contrasts with the topology of another coordination complex showing polycatenation of hydrogen-bonded (4,4) supramolecular grids,

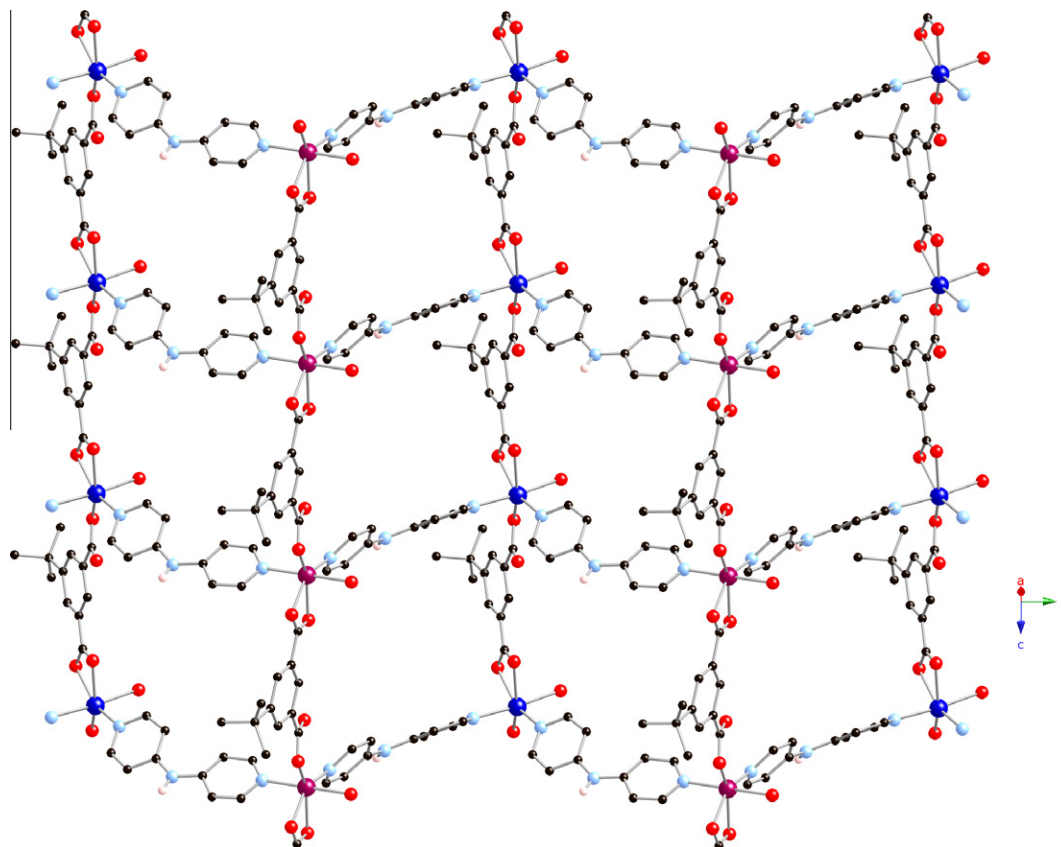


Fig. 2. A single $[\text{Co}(\text{tBuip})(\text{dpa})(\text{H}_2\text{O})]_n$ layer in **1**.

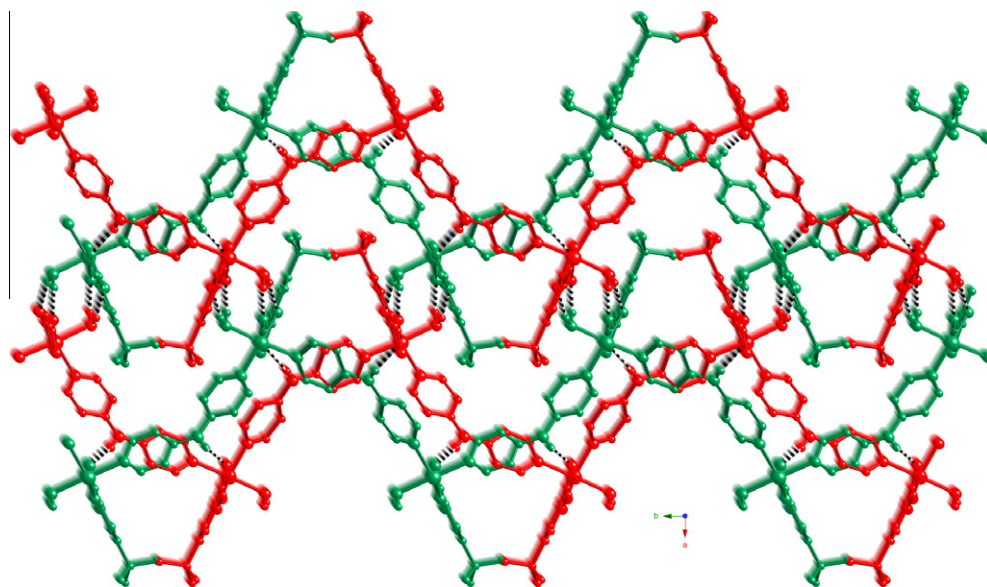


Fig. 3. Interpenetration and stacking of $[\text{Co}(\text{tBuip})(\text{dpa})(\text{H}_2\text{O})]_n$ layers in **1**. Hydrogen bonding is indicated as dashed lines.

$\{[\text{Pt}(\text{Hinic})_2(\text{inic})_2] \cdot 2\text{H}_2\text{O}\}$ (inic = isonicotinate) [43]. This species possess three orthogonal sets of parallel non-interpenetrated (4,4) grids, forming a $2d + 2d + 2d \rightarrow 3\text{D}$ supramolecular arrangement. The 3-fold parallel interpenetration of **2** falls short of the record level of parallel interpenetration of hydrogen bonded coordination complexes, seen in the 5-fold supramolecular (4,4) grid layers in $[\text{Co}(\text{BPDC})_2(\text{Hdpa})_2]$ (BPDC = biphenyldicarboxylate) [44]. In this previously reported material, the greater length of the

BPDC ligands in comparison to MeOip promotes the generation of larger grid apertures, allowing for a higher level of interpenetration. It is clear that judicious adjustment of the length of the monodentate dicarboxylate ligand in $[\text{Co}(\text{dicarboxylate})_2(\text{Hdpa})_2]$ type coordination complexes can allow a modicum of design of interpenetrated hydrogen bonded networks. Three-fold interpenetrated $[\text{Co}(\text{MeOip})_2(\text{Hdpa})_2]_n$ supramolecular layers in **2** aggregate via hydrogen bonding pathways between central N–H amine

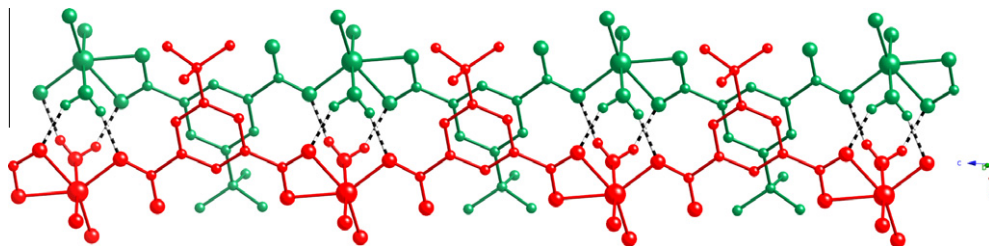


Fig. 4. Close-up view of supramolecular hydrogen-bonding bridged dimeric units in **1**. Hydrogen bonding is indicated as dashed lines.

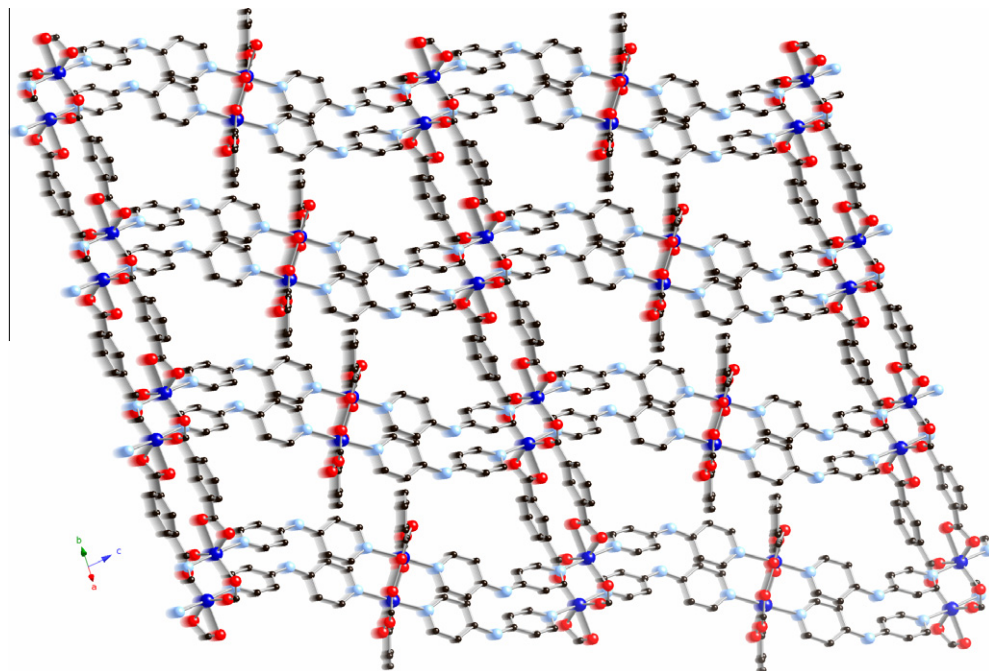


Fig. 5. Three-dimensional $6^5 8$ topology cds network in $[\text{Co}(\text{ip})(\text{dpa})]_n$.

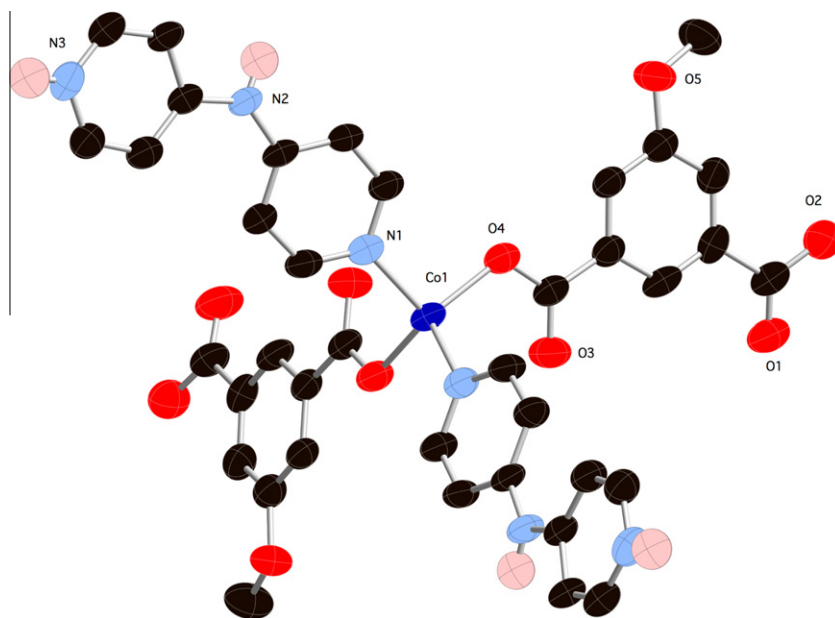


Fig. 6. $[\text{Co}(\text{MeOip})_2(\text{Hdpa})_2]$ coordination complex in **2**.

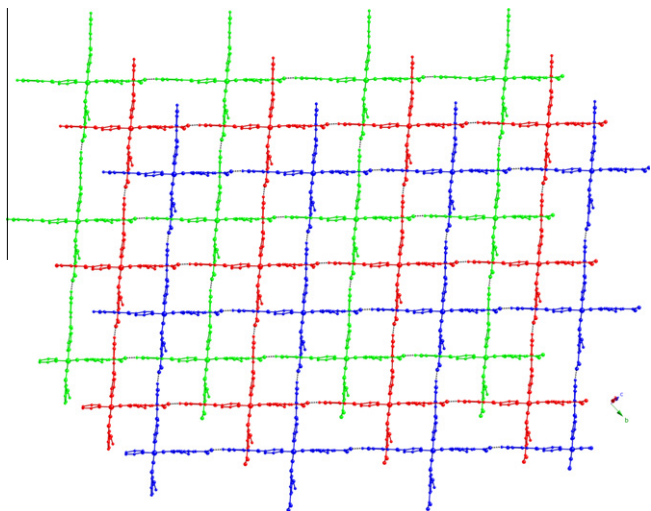


Fig. 7. Three-fold parallel interpenetration of $[\text{Co}(\text{MeOip})_2(\text{Hdpa})_2]_n$ hydrogen-bonded supramolecular layers in **2**.

functional groups of the dpa ligands, and unligated MeOip carboxylate oxygen atoms.

4.4. Structural description of $\{[\text{Co}(\text{OHip})(\text{dpa})(\text{H}_2\text{O})_3]_3 \cdot 2\text{H}_2\text{O}\}_n$ (**3**)

The large asymmetric unit of compound **3** contains three divalent cobalt atoms (Co1, Co2, Co3) with three aqua ligands on each, three dpa ligands, three OHip ligands, and two water molecules of crystallization. One of the water molecules in **3** (O3/O3A) was disordered over bound and unbound positions in a 84/16 ratio. The

coordination environment at each cobalt atom is a distorted $\{\text{CoO}_4\text{N}_2\}$ octahedron, with *cis* disposed dpa pyridyl nitrogen donors, three aqua ligands arranged in a meridional orientation, and an oxygen donor atom from an OHip ligand. Bond lengths and angles within the slightly crystallographically distinct coordination environments are listed in Table S4.

The Co1 atoms are joined by dipodal dpa ligands into $[\text{Co}(\text{OHip})(\text{dpa})(\text{H}_2\text{O})_3]_n$ coordination polymer chains (Fig. 8). As the OHip ligands are monodentate, they serve as pendant groups and do not participate in coordination polymer linkages. The $\text{Co1} \cdots \text{Co1}$ distance through the dpa tethers is 11.410 Å; the pyridyl rings of the dpa ligands are twisted by 44.5° relative to each other. Similarly, the Co2 and Co3 atoms alternate and are bridged by dpa ligands within crystallographically distinct $[\text{Co}(\text{OHip})(\text{dpa})(\text{H}_2\text{O})_3]_n$ chains, but with $\text{Co} \cdots \text{Co}$ distances of 11.477 and 11.506 Å, respectively. The different metal–metal contact distances are enforced by the variances in the dihedral angles between dpa pyridyl rings (42.9° and 46.4° , respectively). All $[\text{Co}(\text{OHip})(\text{dpa})(\text{H}_2\text{O})_3]_n$ chains within **3** are oriented parallel to the *b* crystal direction.

Neighboring chains are aggregated by supramolecular hydrogen bonding between OHip hydroxyl groups and aqua ligands, and also between aqua ligands and unligated OHip carboxylate groups (Fig. 9). Water molecules of crystallization occupy 2.1% of the unit cell volume, and are anchored to the coordination polymer chains by hydrogen bonding acceptance from the dpa central amine functional groups. Some data regarding the extensive hydrogen bonding interactions in **3** is listed in Table S2.

4.5. Structural description of $\{[\text{Co}(\text{mip})(\text{dpa})] \cdot 3\text{H}_2\text{O}\}_n$ (**4**)

The asymmetric unit of compound **4** contains a divalent cobalt atom, a fully deprotonated mip ligand, a dpa ligand, and three

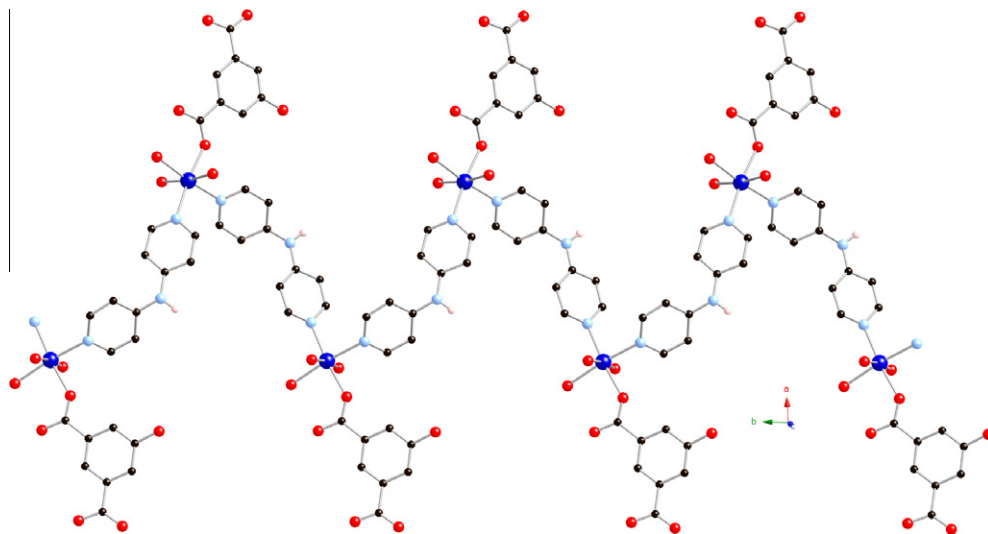


Fig. 8. A single $[\text{Co}(\text{OHip})(\text{dpa})(\text{H}_2\text{O})_3]_n$ coordination polymer chain in **3**.

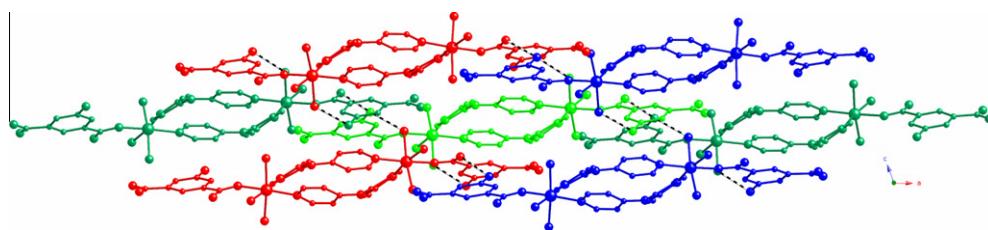


Fig. 9. Supramolecular hydrogen bonding between neighboring chains in **3** (dashed lines).

water molecules of crystallization, one of which is disordered. A distorted $\{\text{CoO}_4\text{N}_2\}$ octahedral coordination environment exists at cobalt, with dpa pyridyl nitrogen donors in the axial positions. Within the equatorial plane lie a chelating mip carboxylate group and two *cis* oxygen donors from two other mip ligands. Bond lengths and angles within the coordination sphere are listed in Table S5.

Exotridentate mip ligands with a $\mu_3\text{-}\kappa^4\text{-O,O':O'':O'''}$ binding mode connect cobalt ions in **4** into $[\text{Co}(\text{mip})]_n$ chains with embedded *anti-syn* bridged $\{\text{Co}_2(\text{OCO})_2\}$ dinuclear kernels (Fig. 10). These dinuclear units alternate with $\{\text{Co}_2(\text{OC}_5\text{O})_2\}$ 16-membered circuits along the chain motifs. The $\text{Co}\cdots\text{Co}$ through-space distances across the dinuclear kernels and larger circuits are 4.020 and 7.558 Å, respectively. Orthogonally disposed sets of parallel $[\text{Co}(\text{mip})]_n$ chains are arranged along the $[1\bar{1}0]$ and $[110]$ crystal directions, linked by pairs of dpa ligands into a 3-D $[\text{Co}(\text{mip})(\text{dpa})]_n$ coordination polymer network (Fig. 11a). The $\text{Co}\cdots\text{Co}$ contact distance through the dpa ligands, which have an inter-ring dihedral angle of 34.9° , is 11.577 Å. If the $\{\text{Co}_2(\text{OCO})_2\}$ dinuclear units are considered 4-connected nodes, the topology of **4** is that of a 6^58 **cds** network (Fig. 11b). This relatively uncommon 3-D topology was encountered in the previously reported unsubstituted isophthalate analog of **4**, $[\text{Co}(\text{ip})(\text{dpa})]\cdot 3\text{H}_2\text{O}$ [40]. Apparently the small steric bulk and the lack of hydrogen-bonding facility of the methyl group in the mip ligand result in an inability to alter coordination polymer topology from that of the unsubstituted isophthalate derivative. Water molecules of crystallization occupy incipient 1-D channels, totaling 22.7% of the unit cell volume, situated between the dpa ligand pairs.

4.6. Structural description of $[\text{Co}(\text{H}_2\text{O})_4(\text{Hdpa})_2](\text{nip})_2\cdot 2\text{H}_2\text{O}$ (**5**)

The asymmetric unit of compound **5** contains two divalent cobalt atoms on crystallographic inversion centers, four aqua ligands, two singly protonated Hdpa ligands, two unligated nip dianions, and two water molecules of crystallization. At each crystallographically distinct cobalt atom, there is a $\{\text{CoO}_4\text{N}_2\}$ octahedral coordination environment, with *trans* Hdpa pyridyl nitrogen donor atoms in axial positions and four aqua ligands in the equatorial planes. Bond lengths and angles within the coordination spheres are listed in Table S6.

In contrast to the *t*Buip, OHip, and mip coordination polymers discussed earlier, compound **5** is a simple coordination cation/anion salt-like complex. Here, isolated $[\text{Co}(\text{H}_2\text{O})_4(\text{Hdpa})_2]^{4+}$ cations and nip anions form chain motifs (Fig. 12) through strong $\text{N-H}\cdots\text{O}^-$ charge-separated hydrogen-bonding between the protonated pyridyl groups of the Hdpa ligands and nip carboxylate oxygen atoms. Other nip anions are anchored to the coordination complex cations by hydrogen bonding acceptance from aqua ligands at carboxylate oxygen atom lone pairs. In turn these chains construct the supramolecular 3-D crystal structure through additional hydrogen bonding patterns involving the central amine

functional groups of the Hdpa ligands, aqua ligands, nip carboxylate groups, and water molecules of crystallization. Detailed information regarding the myriad hydrogen bonding pathways within the coordination complex salt **5** can be found in Table S2 in the Supplementary information. Protonation of one of the pyridyl rings of the dpa precursors results in monodentate pendant Hdpa ligands, preventing aggregation into a higher dimensionality coordination polymer.

4.7. Structural description of $[\text{Co}(\text{sip})(\text{Hdpa})(\text{H}_2\text{O})_4]\cdot 2\text{H}_2\text{O}$ (**6**)

According to single crystal X-ray diffraction, compound **6** is a simple neutral $[\text{Co}(\text{sip})(\text{Hdpa})(\text{H}_2\text{O})_4]$ coordination complex with a slightly distorted octahedral coordination at cobalt. The sip and singly protonated Hdpa ligands are disposed in a *cis* orientation, while the remaining four coordination sites are filled by aqua ligands. The sip ligand is bound to cobalt through one of its carboxylate groups, in a monodentate fashion. Relevant bond lengths and angles within the coordination sphere are given in Table S7.

Charge balance is provided by the protonated pyridyl rings of the Hdpa ligands, which also connect neighboring coordination complexes into supramolecular chains via $\text{N-H}\cdots\text{O}^-$ hydrogen bonding donation to unligated sip carboxylate groups. These same unligated sip carboxylate oxygen atoms accept hydrogen bonding from aqua ligands in neighboring chains, thereby forming supramolecular layers arranged in the *ac* crystal planes (Fig. 13). Central amine groups of the Hdpa ligands promote aggregation into the full supramolecular 3-D crystal structure. Hydrogen bonding information is listed in Table S2. It appears that coordination polymer generation is curtailed during the self-assembly of **6** by protonation of one of the dpa pyridyl rings, as well as the poor ligating ability of the diffusely charged sip sulfonate group. The ability of one of the sip carboxylate groups to bind to cobalt is also likely reduced by its dual hydrogen bonding acceptance.

4.8. Thermogravimetric analysis

According to thermogravimetric analysis (TGA), the aqua ligands of **1** were ejected between ~ 105 and ~ 210 °C, as evidenced by a 3.6% observed mass loss (3.8% calc). The mass then remained stable until ~ 325 °C, where ligand pyrolysis ensued. The 17.0% remnant at ~ 400 °C corresponded well with a deposition of CoO (16.0% calc). For compound **2**, the mass remained stable until ~ 305 °C, where all ligands were combusted in a two-step process. The 10.6% remnant at ~ 450 °C matched roughly with a deposition of CoO (9.5% calc) with some remaining carbon-containing components. Dehydration of **4** occurred from 25 to ~ 100 °C, with a mass loss of 9.7% (11.8% calc); it is likely that some water loss occurred on standing. The mass of **4** then remained nearly constant to ~ 370 °C. Although phase transformations cannot be ruled out completely, it is plausible that the 3-D coordination polymer framework of the **cds** network results in enhanced thermal

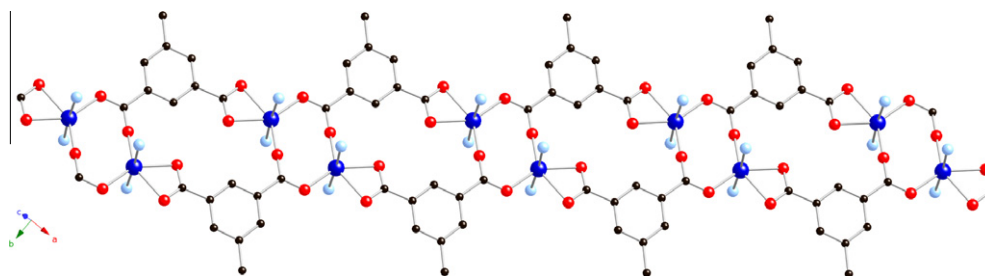


Fig. 10. $[\text{Co}(\text{mip})]_n$ chain in **4**.

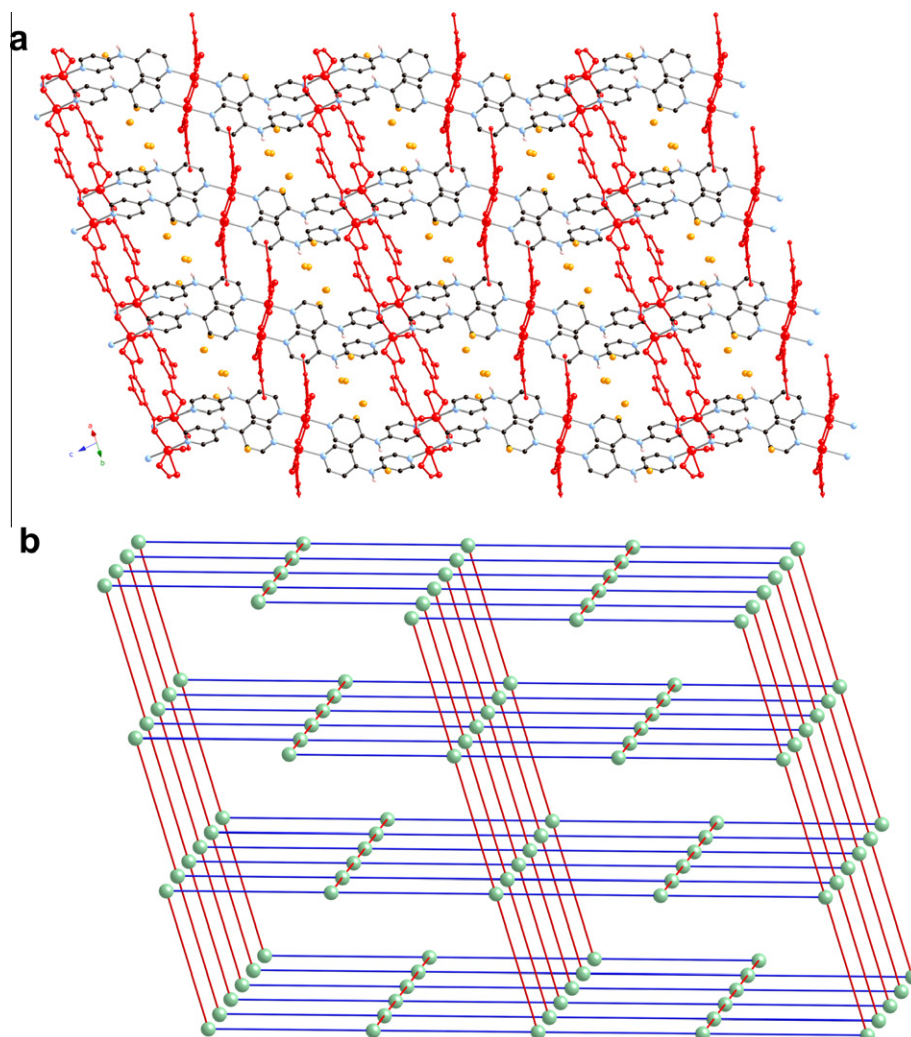


Fig. 11. (a) $[\text{Co}(\text{mip})(\text{dpa})]_n$ network in **4**. $[\text{Co}(\text{mip})]_n$ chains and water molecules of crystallization are shown in red and orange in the online version of this article, respectively. (b) Schematic representation of the 6^58 cds network topology of **4**. The spheres represent the 4-connected $\{\text{Co}_2(\text{OCO})_2\}$ dinuclear units, with mip and dpa connections rendered in red and blue, respectively. (For interpretation of the references to color in this figure legend, the reader is referred to the web version of this paper.)

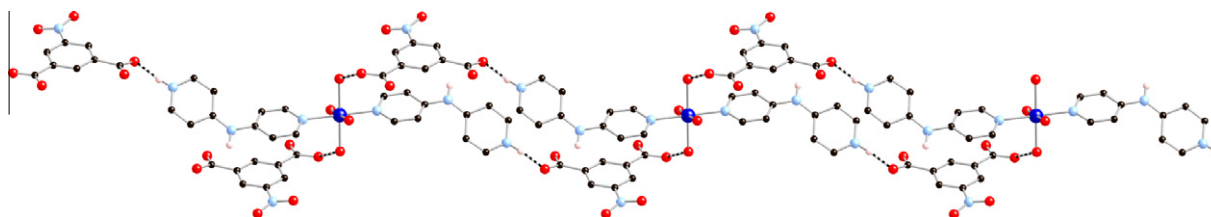


Fig. 12. Supramolecular chain of $[\text{Co}(\text{H}_2\text{O})_4(\text{Hdpa})_2]^{4+}$ complex cations and nip anions in **5**. Hydrogen bonding is indicated as dashed lines.

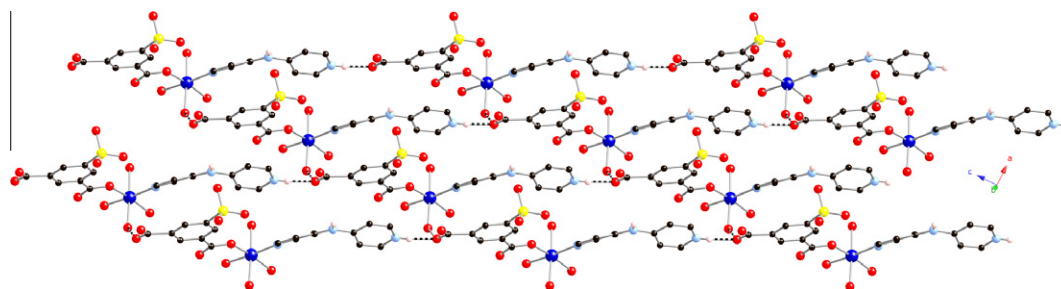


Fig. 13. Supramolecular layer of $[\text{Co}(\text{sip})(\text{Hdpa})(\text{H}_2\text{O})_4]$ neutral coordination complexes in **6**.

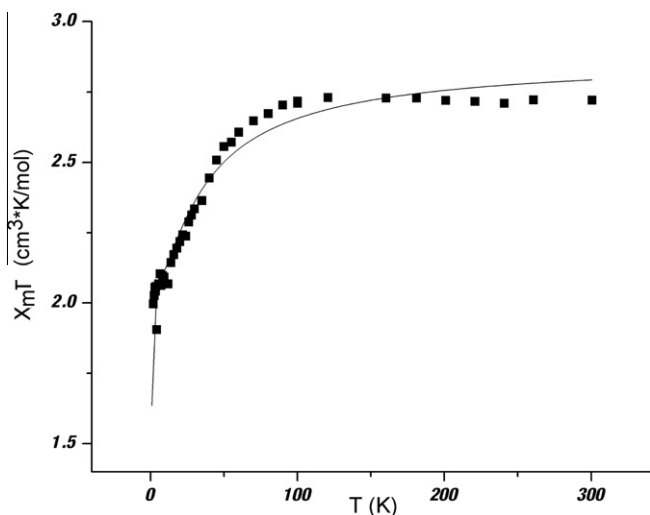


Fig. 14. Variable temperature magnetic data for **1**. The best fit to Eq. (1) in the text is drawn as a thin black line.

stability. Ligand ejection occurred above 370 °C, which was incomplete by the end of the experiment at 480 °C. The 39.6% mass remnant is consistent with a deposition of CoCO₃ (25.7% calc) and uncombusted organics. Thermograms for **1**, **2**, and **4** are shown in Figs. S1–S3, respectively.

4.9. Variable temperature magnetic properties of **1** and **4**

The magnetic susceptibility of **1** and **4** as a function of temperature was measured in order to investigate the possibility of hydrogen-bonding or carboxylate-bridge mediated magnetic superexchange. As mentioned previously, pairwise Co–O–H···O–Co supramolecular contacts are present in **1**, whose metal atoms are slightly less than 5 Å apart. The $\chi_m T$ product value for **1** at 300 K was 2.72 cm³-K mol Co⁻¹. Upon cooling the $\chi_m T$ value decreased very slowly, dropping to 2.65 cm³-K mol Co⁻¹ at 70 K, 2.33 cm³-K mol Co⁻¹ at 30 K, and 2.00 cm³-K mol Co⁻¹ at 2 K. The inverse susceptibility data were fit over the entire temperature range to the Curie-Weiss law (Fig. S4), yielding $C = 2.75$ cm³-K mol Co⁻¹ and $\Theta = -3.2$ K. Although the negative value for Θ portends antiferromagnetic coupling, care must be taken in this interpretation because of the likelihood of zero-field splitting in distorted octahedral $S = 3/2$ coordination environments [45]. The phenomenological expression of Rueff (Eq. (1)) [46] was used to model the variable temperature magnetic data for **1** to estimate the competing effects of antiferromagnetic superexchange (J) and zero-field splitting (D). Best-fit values (Fig. 13) were $A = 0.71(4)$ cm³-K mol Co⁻¹ and $B = 2.16(3)$ cm³-K mol Co⁻¹ giving $g = 2.47(4)$, $D = 24(3)$ cm⁻¹, and $J = -0.19(2)$ cm⁻¹ with $R = \{\sum[(\chi_m T)_{\text{obs}} - (\chi_m T)_{\text{calc}}]^2 / \sum[(\chi_m T)_{\text{obs}}]^2\} = 3.71 \times 10^{-3}$. The small, negative J value indicates very weak antiferromagnetic hydrogen-bonding mediated coupling between cobalt ions in different coordination polymer layers, consistent with literature precedent [47].

$$\chi_m T = A \exp(-D/kT) + B \exp(J/kT)$$

where

$$A + B = C = (5Ng^2\beta^2/4k) \quad (1)$$

For **4**, which possesses *anti-syn* bridged {Co₂(OCO)₂} dinuclear kernels, the $\chi_m T$ product value for **1** at 300 K was 3.19 cm³-K mol Co⁻¹. The $\chi_m T$ value decreased slowly upon cooling (Fig. 15), reaching 3.13 cm³-K mol Co⁻¹ at 100 K and 2.84 cm³-K mol Co⁻¹ at 50 K. Below this temperature the $\chi_m T$ product decayed more rapidly,

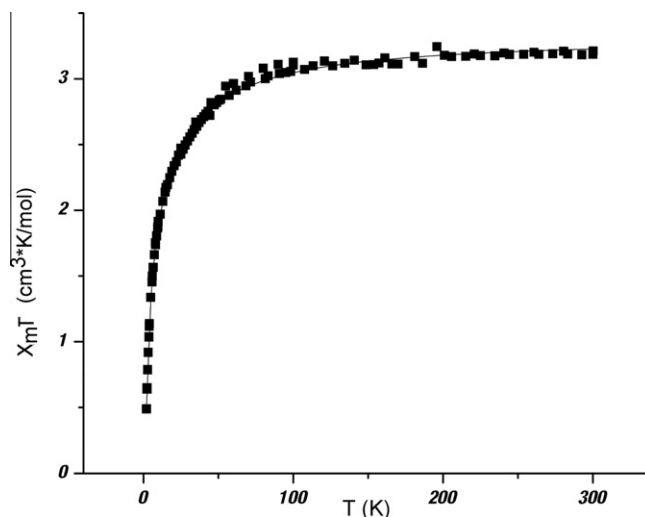


Fig. 15. Variable temperature magnetic data for **4**. The best fit to Eq. (1) in the text is drawn as a thin black line.

finally reaching 0.49 cm³-K mol Co⁻¹ at 2 K. The inverse susceptibility data were fit to the Curie-Weiss law (Fig. S5), giving $C = 3.29$ cm³-K mol Co⁻¹ and $\Theta = -8.0$ K. The $\chi_m T$ behavior and larger Weiss constant possibly indicates stronger antiferromagnetic coupling than that seen in **1**. The Rueff model was once again applied, giving best-fit values (Fig. 14) of $A = 0.76(3)$ cm³-K mol Co⁻¹ and $B = 2.57(3)$ cm³-K mol Co⁻¹ giving $g = 2.72(3)$, $D = 21(1)$ cm⁻¹, and $J = -2.27(4)$ cm⁻¹ with $R = 1.01 \times 10^{-3}$. It is apparent that the dual carboxylate bridges between $S = 3/2$ ions in **4** promotes stronger antiferromagnetic coupling than that afforded by the hydrogen-bonding mediated exchange pathway in **1**. In both cases the magnitude of the zero-field splitting is largely the same, given similar coordination environments.

5. Conclusions

The dimensionality of cobalt isophthalate coordination polymers containing 4,4'-dipyridylamine depends critically upon the steric hindrance or hydrogen-bonding facility of any 5-position isophthalate substituents. Substituents with a small degree of steric bulk (hydrogen, methyl) permits generation of uncommon 3-D 4-connected 6⁵⁸ **cdfs** networks, based on antiferromagnetically coupled *anti-syn* bridged {Co₂(OCO)₂} dinuclear units. Bulkier substituents (*tert*-butyl, methoxy) tend to reduce coordination polymer dimensionality, consistent with some recent literature precedent. Substituents that can participate in hydrogen bonding, such as nitro, hydroxy, and sulfonate groups, can promote formation of simple coordination complexes via ample hydrogen bonding pathways. It is clear that deliberate alteration of 5-position substituents within isophthalate-type ligands can provide a modicum of crystal design in this system.

Acknowledgments

Financial support for this work was provided by the donors of the American Chemical Society Petroleum Research Fund (Type B Grant for undergraduate research). C.M.G. thanks the Michigan State University Honors College for his Professorial Assistantship.

Appendix A. Supplementary material

CCDC 809642, 809641, 813224, 815145, 815423, and 815840 contain the supplementary crystallographic data for **1–6**. These

data can be obtained free of charge from The Cambridge Crystallographic Data Centre via www.ccdc.cam.ac.uk/data_request/cif. Metrical parameters for bond lengths, bond angles, and hydrogen-bonding are given in Tables S1–S7. Additional thermogravimetric analysis and magnetic data figures are also given in Figures S1–S5. Supplementary data associated with this article can be found, in the online version, at [doi:10.1016/j.ica.2011.09.016](https://doi.org/10.1016/j.ica.2011.09.016).

References

- [1] (a) C. Janiak, *Dalton Trans.* (2003) 2781 (and references therein); (b) U. Mueller, M. Schubert, F. Teich, H. Puetter, K. Schierle-Arndt, J. Pastré, *J. Mater. Chem.* 16 (2006) 626; (c) A.U. Czaja, N. Trukhan, U. Müller, *Chem. Soc. Rev.* 38 (2009) 1284 (and references therein); (d) C. Janiak, J.K. Vieth, *New J. Chem.* 34 (2010) 2366.
- [2] (a) L. Pan, D.H. Olson, L.R. Ciemnomolowski, R. Heddy, J. Li, *Angew. Chem., Int. Ed.* 45 (2006) 616; (b) M. Dinca, A.F. Yu, J.R. Long, *J. Am. Chem. Soc.* 128 (2006) 8904; (c) J.L.C. Roswell, O.M. Yaghi, *Angew. Chem., Int. Ed.* 44 (2005) 4670; (d) R. Matsuda, R. Kitaura, S. Kitagawa, Y. Kubota, R.V. Belosludov, T.C. Kobayashi, H. Sakamoto, T. Chiba, M. Takata, Y. Kawazoe, Y. Mita, *Nature* 436 (2005) 238; (e) A.C. Sudik, A.R. Millward, N.W. Ockwig, A.P. Côté, J. Kim, O.M. Yaghi, *J. Am. Chem. Soc.* 127 (2005) 7110; (f) X. Zhao, B. Xiao, A.J. Fletcher, K.M. Thomas, D. Bradshaw, M.J. Rosseinsky, *Science* 306 (2004) 1012; (g) N.L. Rosi, J. Eckert, M. Eddaoudi, D.T. Vodak, J. Kim, M. O'Keefe, O.M. Yaghi, *Science* 300 (2003) 1127; (h) G. Férey, M. Latroche, C. Serre, F. Millange, T. Loiseau, A. Percheron-Guegan, *Chem. Commun.* (2003) 2976; (i) H. Li, M. Eddaoudi, M. O'Keefe, O.M. Yaghi, *Nature* 402 (1999) 276.
- [3] (a) J.-R. Li, R.J. Kuppler, H.-C. Zhou, *Chem. Soc. Rev.* 38 (2009) 1477 (and references therein); (b) A. Cingolani, S. Galli, N. Masciocchi, L. Pandolfo, C. Pettinari, A. Sironi, *Chem. Eur. J.* 14 (2008) 9890; (c) J.S. Seo, D. Whang, H. Lee, S.I. Jun, J. Oh, Y.J. Jeon, K. Kim, *Nature* 404 (2000) 982; (d) A. Mallick, S. Saha, P. Pachfule, S. Roy, R. Banerjee, *J. Mater. Chem.* 20 (2010) 9073.
- [4] (a) Q.-R. Fang, G.-S. Zhu, M. Xue, J.-Y. Sun, S.-L. Qiu, *Dalton Trans.* (2006) 2399; (b) X.-M. Zhang, M.-L. Tong, H.K. Lee, X.-M. Chen, *J. Solid State Chem.* 160 (2001) 118; (c) O.M. Yaghi, H. Li, T.L. Groy, *Inorg. Chem.* 36 (1997) 4292.
- [5] (a) J.Y. Lee, O.K. Farha, J. Roberts, K.A. Scheidt, S.T. Nguyen, J.T. Hupp, *Chem. Soc. Rev.* 38 (2009) 1450 (and references therein); (b) L. Ma, C. Abney, W. Lin, *Chem. Soc. Rev.* 38 (2009) 1248; (c) S.G. Baca, M.T. Reetz, R. Goddard, I.G. Philippova, Y.A. Simonov, M. Gdaniec, N. Gerbeleu, *Polyhedron* 25 (2006) 1215; (d) H. Han, S. Zhang, H. Hou, Y. Fan, Y. Zhu, *Eur. J. Inorg. Chem.* 8 (2006) 1594; (e) C.-D. Wu, A. Hu, L. Zhang, W. Lin, *J. Am. Chem. Soc.* 127 (2005) 8940; (f) W. Mori, S. Takamizawa, C.N. Kato, T. Ohmura, T. Sato, *Micropor. Mesopor. Mater.* 73 (2004) 31; (g) N. Guillou, Q. Gao, P.M. Forster, J.S. Chang, M. Nogués, S.-E. Park, G. Férey, A.K. Cheetham, *Angew. Chem., Int. Ed.* 40 (2001) 2831.
- [6] (a) H.A. Habib, A. Hoffmann, H.A. Höpfe, G. Steinfeld, C. Janiak, *Inorg. Chem.* 48 (2009) 2166; (b) W. Chen, J.Y. Wang, C. Chen, Q. Yue, H.M. Yuan, J.S. Chen, S.N. Wang, *Inorg. Chem.* 42 (2003) 944; (c) N. Hao, E. Shen, Y.B. Li, E.B. Wang, C.W. Hu, L. Xu, *Eur. J. Inorg. Chem.* (2004) 4102.
- [7] (a) S. Zang, Y. Su, Y. Li, Z. Ni, Q. Meng, *Inorg. Chem.* 45 (2006) 174; (b) L. Wang, M. Yang, G. Li, Z. Shi, S. Feng, *Inorg. Chem.* 45 (2006) 2474.
- [8] (a) M. Eddaoudi, J. Kim, N. Rosi, D. Vodak, J. Wachter, M. O'Keefe, O.M. Yaghi, *Science* 295 (2002) 469; (b) X.-N. Cheng, W.-X. Zhang, Y.-Y. Lin, Y.-Z. Zheng, X.-M. Chen, *Adv. Mater.* 19 (2007) 1494.
- [9] (a) J. Tao, M.L. Tong, X.M. Chen, *J. Chem. Soc., Dalton Trans.* (2000) 3669; (b) S.A. Bourne, J. Lu, B. Moulton, M.J. Zaworotko, *Chem. Commun.* (2001) 861; (c) J. Tao, X.M. Chen, R.B. Huang, L.S. Zhen, *J. Solid State Chem.* 170 (2003) 130.
- [10] (a) B. Chen, C. Liang, J. Yang, D.S. Contreras, Y.L. Clancy, E.B. Lobkovsky, O.M. Yaghi, S. Dai, *Angew. Chem., Int. Ed.* 45 (2006) 1390; (b) S.W. Lee, H.J. Kim, Y.K. Lee, K. Park, J.H. Son, Y. Kwon, *Inorg. Chim. Acta* 353 (2003) 151.
- [11] M. Kurmoo, *Chem. Soc. Rev.* 38 (2009) 1353 (and references therein).
- [12] X.J. Li, R. Cao, W.H. Bi, Y.Q. Wang, Y.L. Wang, X. Li, *Polyhedron* 24 (2005) 2955.
- [13] H.Y. He, Y.L. Zhou, Y. Hong, L.G. Zhu, *J. Mol. Struct.* 737 (2005) 97.
- [14] X.J. Li, X.Y. Wang, S. Gao, R. Cao, *Inorg. Chem.* 45 (2006) 1508.
- [15] R.K. Feller, A.K. Cheetham, *Dalton Trans.* (2008) 2034.
- [16] L.F. Ma, B. Li, X.Y. Sun, L.Y. Wang, Y.T. Fan, *Z. Anorg. Allg. Chem.* 636 (2010) 1606.
- [17] Z.M. Wilseck, C.M. Gandolfo, R.L. LaDuca, *Inorg. Chim. Acta* 363 (2010) 3865.
- [18] M. Du, Z.H. Zhang, Y.P. You, X.J. Zhao, *CrystEngComm* 10 (2008) 306.
- [19] J. Luo, M. Hong, R. Wang, R. Cao, L. Han, D. Yuan, Z. Lin, Y. Zhou, *Inorg. Chem.* 42 (2003) 4486.
- [20] Y. Liu, Q. He, X. Zhang, Z. Xue, C. Lv, *Acta Crystallogr., Sect. E* 64 (2008) m1605.
- [21] F. Wang, K.J. Deng, G.Y. Lai, L. Cao, L.L. Wen, D.F. Li, J. Inorg. Organomet. Polym. 19 (2009) 494.
- [22] L.K. Sposato, R.L. LaDuca, *Acta Crystallogr., Sect. E* 65 (2009) m1082.
- [23] L. Pan, B. Parker, X. Huang, D.H. Olson, J. Lee, J. Li, *J. Am. Chem. Soc.* 128 (2006) 4180.
- [24] Z. Zhang, S. Chen, J. Mi, M. He, Q. Chen, M. Du, *Chem. Commun.* 46 (2010) 8427.
- [25] B. Xu, G. Li, H. Yang, S. Gao, R. Cao, *Inorg. Chem. Commun.* 14 (2011) 493.
- [26] (a) Q.Y. Liu, D.Q. Yuan, L. Xu, *Cryst. Growth Des.* 7 (2007) 1832; (b) C. Gandolfo, R.L. LaDuca, *Cryst. Growth Des.* 11 (2011) 1328.
- [27] T. Fukushima, S. Horike, Y. Inubushi, K. Nakagawa, Y. Kubota, M. Takata, S. Kitagawa, *Angew. Chem., Int. Ed.* 49 (2010) 4820.
- [28] D.S. Zhou, F.K. Wang, S.Y. Yang, Z.X. Xie, R.B. Huang, *CrystEngComm* 11 (2009) 2548.
- [29] Z.M. Wilseck, C.M. Gandolfo, R.L. LaDuca, *Inorg. Chim. Acta* 363 (2010) 3865.
- [30] M.R. Montney, S. Mallika Krishnan, N.M. Patel, R.M. Supkowski, R.L. LaDuca, *Cryst. Growth Des.* 7 (2007) 1145.
- [31] E. Shyu, R.M. Supkowski, R.L. LaDuca, *Inorg. Chem.* 48 (2009) 2723.
- [32] R.L. LaDuca, *Coord. Chem. Rev.* 253 (2009) 1759.
- [33] P.J. Zapf, R.L. LaDuca, R.S. Rarig, K.M. Johnson, J. Zubieta, *Inorg. Chem.* 37 (1998) 3411.
- [34] O. Kahn, *Molecular Magnetism*, VCH Publishers, New York, 1993.
- [35] SAINT, Software for Data Extraction and Reduction, Version 6.02 Bruker AXS, Inc., Madison, WI, 2002.
- [36] SADABS, Software for Empirical Absorption Correction, Version 2.03 Bruker AXS, Inc., Madison, WI, 2002.
- [37] G.M. Sheldrick, SHELXL, Program for Crystal Structure Refinement, University of Göttingen, Göttingen, Germany, 1997.
- [38] G.M. Sheldrick, CELLNOW, University of Göttingen, Göttingen, Germany, 2003.
- [39] M. Kurmoo, C. Estournes, Y. Oka, H. Kumagai, K. Inoue, *Inorg. Chem.* 44 (2005) 217.
- [40] K.M. Blake, M.A. Braverman, J.H. Nettleman, L.K. Sposato, R.L. LaDuca, *Inorg. Chim. Acta* 363 (2010) 3966.
- [41] T. Steiner, *Angew. Chem., Int. Ed.* 41 (2002) 48.
- [42] H.B. Burgi, J.D. Dunitz, *Acc. Chem. Res.* 16 (1983) 153.
- [43] C.B. Aakeröy, A.M. Beatty, D.S. Leinen, *Angew. Chem., Int. Ed.* 38 (1999) 1815.
- [44] M.R. Montney, R.M. Supkowski, R.L. LaDuca, *CrystEngComm* 10 (2008) 111.
- [45] R.L. Carlin, *Magnetochemistry*, Springer-Verlag, Berlin, 1986.
- [46] J.M. Rueff, N. Masciocchi, P. Rabu, A. Sironi, A. Skoulios, *Eur. J. Inorg. Chem.* (2001) 2843.
- [47] (a) C. Desplanches, E. Ruiz, A. Rodríguez-Fortea, S. Alvarez, *J. Am. Chem. Soc.* 124 (2002) 5197; (b) M. Ardon, A. Bino, K. Michelsen, E. Pedersen, *J. Am. Chem. Soc.* 109 (1987) 5585; (c) U. Bosek, K. Wieghardt, B. Nuber, J. Weiss, *Angew. Chem., Int. Ed.* 29 (1990) 1055; (d) P.A. Goodson, J. Glerup, D.J. Hodgson, K. Michelsen, U. Rychlewski, *Inorg. Chem.* 33 (1994) 359.